APPENDIX B

Attrition Assessment for Slurry Bubble Column Reactor Catalysts

ABSTRACT

Significant interest in 3-phase slurry bubble column reactors (SBCRs) has come about in recent years due to their excellent heat removal capabilities during reaction. However, no evaluation test for catalyst attrition resistance is available in the literature yet for SBCR catalysts, although severe attrition of catalyst particles has actually been encountered in SBCRs. In this work, fluidized bed catalyst attrition tests (fluidized bed and jet cup) and other tests (collision and ultrasound) are evaluated for the first time for their suitability in predicting catalyst attrition in an SBCR. Based on comparisons of particle morphology and size distribution (PSD) of a silica supported cobalt catalyst before and after use in an SBCR with the results from the various attrition assessment tests, it is suggested that the fluidized bed, jet cup and ultrasound tests all provide reasonable and efficient predictions of catalyst attrition. Although the dominant attrition mechanism appeared to be fracture in both SBCR run and collision test, the latter showed too little attrition efficiency to be suitable as an attrition test. Despite the fact that abrasion occurs to a greater degree during the fluidized bed, jet cup, and ultrasound tests compared to during an SBCR run, all these three tests cause particle breakage similar to that in the SBCR, but in relatively short periods of time. Therefore, all three, especially the jet cup test, are suitable tests for predicting catalyst attrition resistance in an SBCR environment.

1. INTRODUCTION

Attrition, defined as the unwanted breakdown of solid particles [1], is a commonly encountered problem in catalytic chemical reactors, especially fluidized bed types [2]. Attrition resistance is one of the critical parameters in the development of catalysts because any attrition of a catalyst causes loss of the catalytic agent and lower product quality. In fluidized bed reactors, attrition can also cause additional filtration and plugging problems and affect the fluidization properties.

Such problems have stimulated many earlier studies [3-15]. Currently, it is believed that attrition processes include both abrasion/erosion (the process during which particle surface layers or corners are removed) and fracture (the fragmentation of particles) [1,2]. These are due to various types of stresses that catalyst particles undergo during reaction, among which the major ones include contact, thermal, pressure, and chemical stresses [2]. For example, in Fischer-Tropsch synthesis (FTS), phase change and carbon deposition have been suggested to be responsible for the nano-scale breakage of iron catalysts [13]. In most earlier studies, however, only attrition due to hydrodynamic forces has been the focus of the research, whereas the other three sources of stress listed above have been assumed to be negligible. In recent reviews and studies by Ghadiri and coworkers on particle attrition [16-18], particle breakdown during impact has been further categorized into different breakage modes according to the impact velocity, particle size and shape, and contact geometry. Particle fracture during impact due to pre-existing internal or surface flaws is classified as brittle failure. Crack initiation, on the other hand, is considered to be semibrittle failure, which can be further categorized by fragmentation or chipping depending on the position of the cracks.

Based on such understanding of attrition processes, several types of attrition assessment methods have been developed and used to evaluate catalyst attrition resistance [3,4,9-11,19-24]. Since it has been concluded that no single particle can represent all the particles involved [2], most catalyst attrition tests involve multiple particles. While tests have been developed for various reactor configurations, such as the compression [19] and rotating drum [20,21] tests aimed mainly at moving bed reactor catalysts, most tests developed have focused on fluidized bed catalysts, which can undergo extensive attrition due to particle-particle and particle-wall collisions. In order to mimic the particle movement and collision inside fluidized bed reactors, Forsythe and Hertwig [3] were the first to use a high-velocity air jet in their attrition test device. This formed the basis of various subsequent tests [4,9,10,12,22,23], including an ASTM (American Standard Test Method) procedure [24]. In a more recently proposed ASTM method, the jet cup test [11], catalyst particles are also fluidized by a high velocity air jet. As mentioned above, physical attrition properties of the catalyst particles are the only ones measured in these tests.

Significant interest in slurry bubble column reactors (SBCRs) has come about in recent years due to their excellent heat removal capabilities during reaction, especially for exthothermic reactions such as FTS. Although it had been suggested that SBCRs are free of catalyst attrition and erosion problems [25], severe attrition problems have been encountered [26]. Due to the complex nature of attrition in three-phase reactors, the attrition mechanisms in SBCRs are still not clear. A suitable evaluation of catalyst attrition resistance is hence a necessity in the SBCR catalyst development. Although, the rotating drum test was modified in order to test a slurry of unsupported precarbided or carbided iron SBCR catalysts in a previous study [15], the results were not compared to attrition in actual SBCR runs. Thus, none of the test methods reported to

date have been developed and qualified for use in assessing the attrition resistance of catalysts for SBCRs.

In the present study, Co/SiO_2 was tested using four different types of attrition assessment methods and the test results were compared to laboratory-scale SBCR results obtained under reaction conditions. The goal was to develop a suitable laboratory test method for predicting the attrition of catalysts under SBCR conditions. Only physical effects have been considered in these comparisons.

2. EXPERIMENT

2.1 Catalyst

The catalyst used was a spray dried silica (Davison Grade 952) supported, Zr promoted, Co catalyst prepared using the incipient wetness technique. After the silica support was pre-calcined at 500°C for 10 hrs and pre-sieved to 38-90 μm (400-170 mesh), Co and Zr salts in an aqueous solution were co-impregnated using incipient wetness in amounts to produce a reduced catalyst having 20 wt% Co and 8.5 wt% Zr. The catalyst precursor was then dried at 115°C for 5 hrs and calcined at 300°C. The prepared catalyst was sieved again after calcination to 38-90 μm using standard sieves. Since particulate materials can undergo size segregation during storage and transportation, such materials have to be mixed as well as possible prior to taking samples. Because the total amount of the catalyst was not very large in this case, this was accomplished by shaking the catalyst container thoroughly in several directions prior to removing a sample.

2.2 Instrumentation and Procedures

2.2.1 SBCR System

The Co catalyst was placed in a 1 inch (1 in = 2.54 cm) diameter, 3 foot (1 foot = 12 in) tall SBCR under Fischer-Tropsch synthesis (FTS) reaction conditions for 240 hrs. All FTS runs

were at 450 psi total pressure (including N_2) and 220-240°C with a CO/H_2 ratio of 2. The slurry initially consisted of Synfluid (Chevron) as the liquid phase and 15 wt% of catalyst presieved to 38-90 μm. After the SBCR run, the catalyst was extracted from the slurry liquid by solvent extraction. The resulting catalyst particles were characterized and compared to those of the catalyst as prepared and sieved.

2.2.2 Air Supply System

Air flow is essential for most of the attrition tests employed. Therefore, a supply system was built in order to supply a steady flow of humidified or nonhumidified air. The flow rate was controlled by a mass flow meter or a rotameter. The humidity and temperature of the airflow was monitored using an on-line Fisher temperature and relative humidity meter. The humidity was able to be adjusted by controlling the volume of air bubbled through a distilled water reservoir.

2.2.3 Collision Test

As illustrated in Figure 1, the instrument for this test consisted of an air supply tube, sealed catalyst reservoir, capillary particle drop channel, and collection assembly. The collection assembly also provided the hard surface (pyrex glass) with which the accelerated particles collided. After loading 1 g of sample into the catalyst reservoir with the air supply tube

Figure 1. Collision or drop shatter system

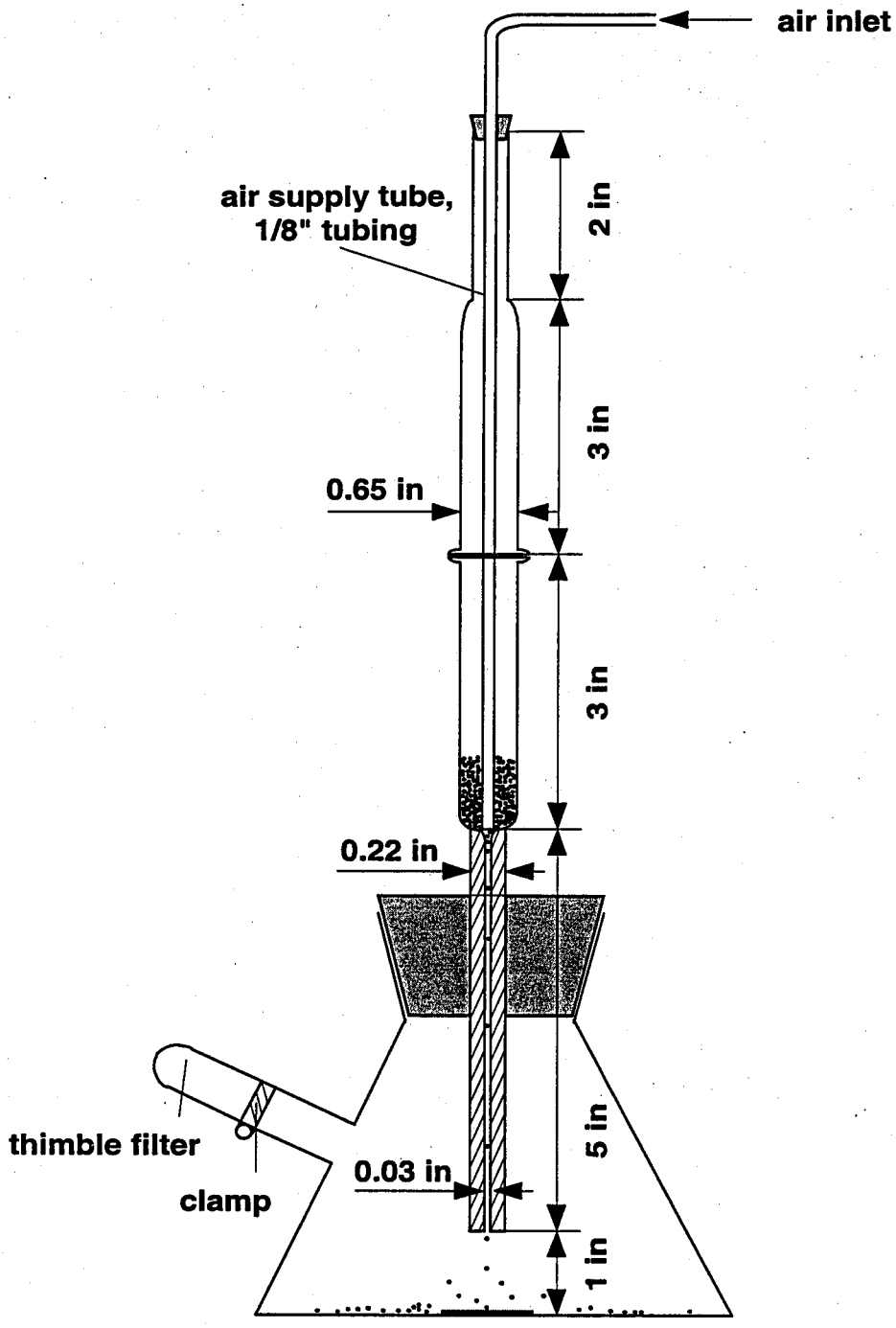

depressed against the entry to the drop channel in order to prevent particle flow out of the reservoir, the reservoir was sealed. After the air jet stabilized at a set flow rate, the air supply tube was raised about 0.5 ± 0.01 mm to provide a gap through which particles could slip into the drop channel. The particles fell into the drop channel and were then accelerated by the air stream before colliding with the inner flat surface of the collection assembly. The speed of the particles striking the hard surfaces was 12 m/s. The gas outlet of the collection assembly was covered with a thimble filter that prevented fine particle loss. The particles collected by the thimble and the collection assembly were removed after the test and analyzed for change in particle size distribution (PSD).

2.2.4 Fluidized Bed Test

A modified fluidized bed test system, based on ASTM D5757-95 [24] but smaller, was employed in this study. This scaled down system is considered superior since less than 5 g of catalyst is required rather than 50 g. The fluidized bed dimensions were calculated using the minimum fluidization gas velocity equation [27]. The gas distributor design was based on the literature [22,23]. The instrument, gas distributor plate and orifice dimensions and setup are illustrated in Figure 2.

In order to prevent the particles from sticking to the tube as a result of static electricity, humidified air (relative humidity of $60 \pm 5\%$) was used as the gas medium instead of using a mechanical tapping system. The fines collection assembly was weighed before the test and its mass recorded. With the air flowing at 0.5 *l*/min and the fines collection assembly removed, 3.0 g of sample were charged into the attrition bed. The fines collection assembly was then replaced and the air flow increased to the desired level. In the procedure given in reference [23], the air

Figure 2. Fluidized bed system

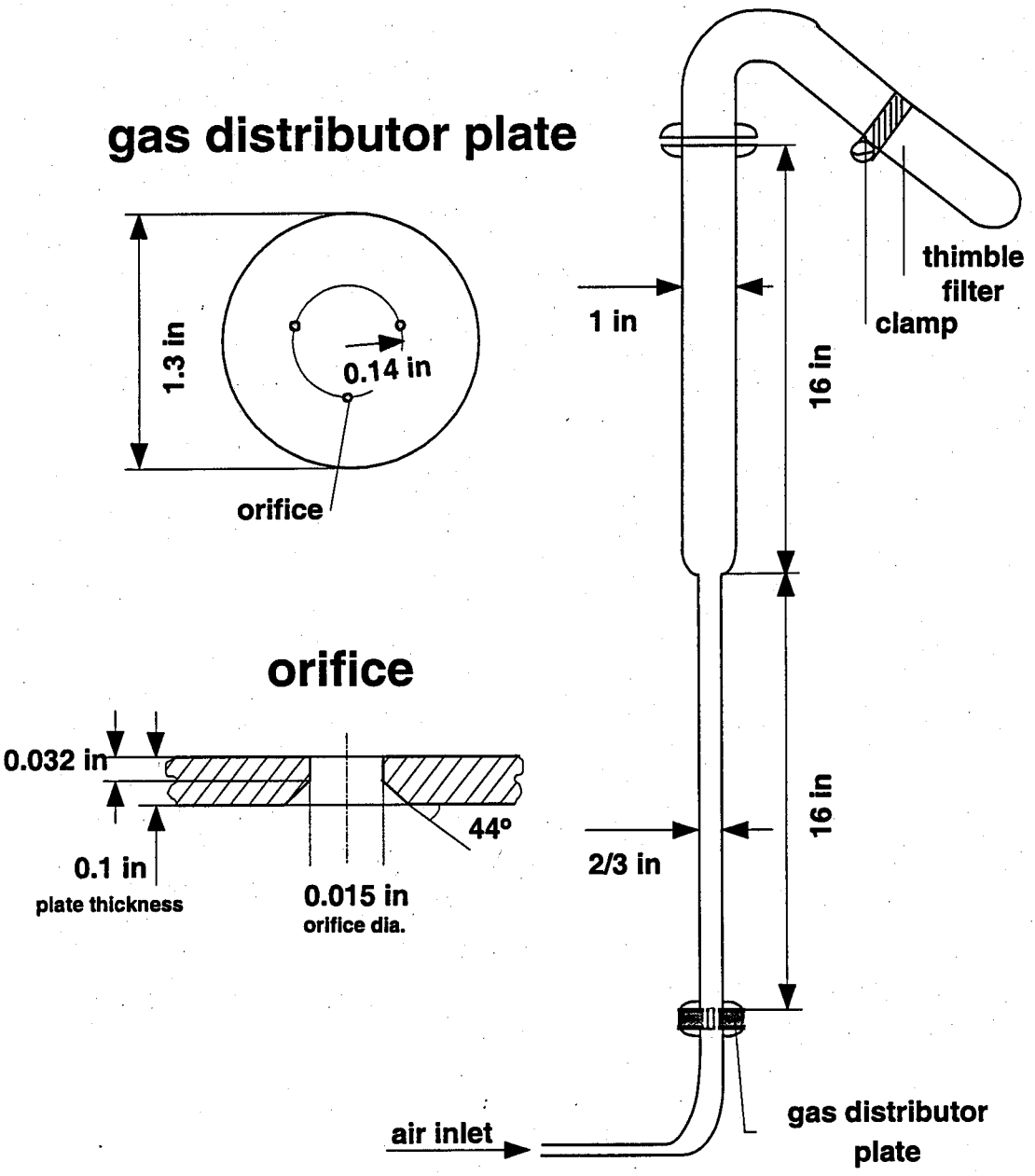

flow is specified to be stopped periodically to measure the rate of loss of fines. However, this potentially leads to turbulence in the fluidization condition and was determined to have an impact on the attrition process inside the fluidized bed. In order to determine the rate of loss of fines without stopping the air flow, two thimbles were weighed and numbered before the experiments in the present study, which is similar to the ASTM procedure [24]. The interchange of thimbles was made quickly to minimize any particle loss. After 6, 12, 18, or 24 hrs time-on-stream, the air supply was stopped. All the catalyst particles were recovered from both the fluidized bed and the fines collection assembly for particle size distribution analysis.

2.2.5 Jet Cup Test

The jet cup test system was based on a proposed ASTM design. As illustrated in Figure 3, the instrument consisted of an air inlet tube connected to the sample cup at the bottom, the settling chamber, and the fines collection assembly. Five grams of sample were weighed and charged into the sample cup. The jet cup was then attached to the settling chamber. After all joints were sealed, humidified air with a relative humidity of $60 \pm 5\%$ was introduced at a controlled flow rate of 10, 15, or 20 *l*/min for one hour. Similar to the fluidized bed test, in order not to interrupt the air flow during experiment, two thimbles were weighted and numbered before the start of the experiment to determine the rate of loss of fines. A thimble, placed on the fines collection assembly, was interchanged with the other quickly at 5 min, 15 min, and 30 min after the start of air flow and its mass recorded. The air flow was stopped after 1 hr on stream, and the fines in the thimbles and the coarse particles in the jet cup were recovered for analysis.

2.2.6 Ultrasonic Test

Figure 3. Jet cup system

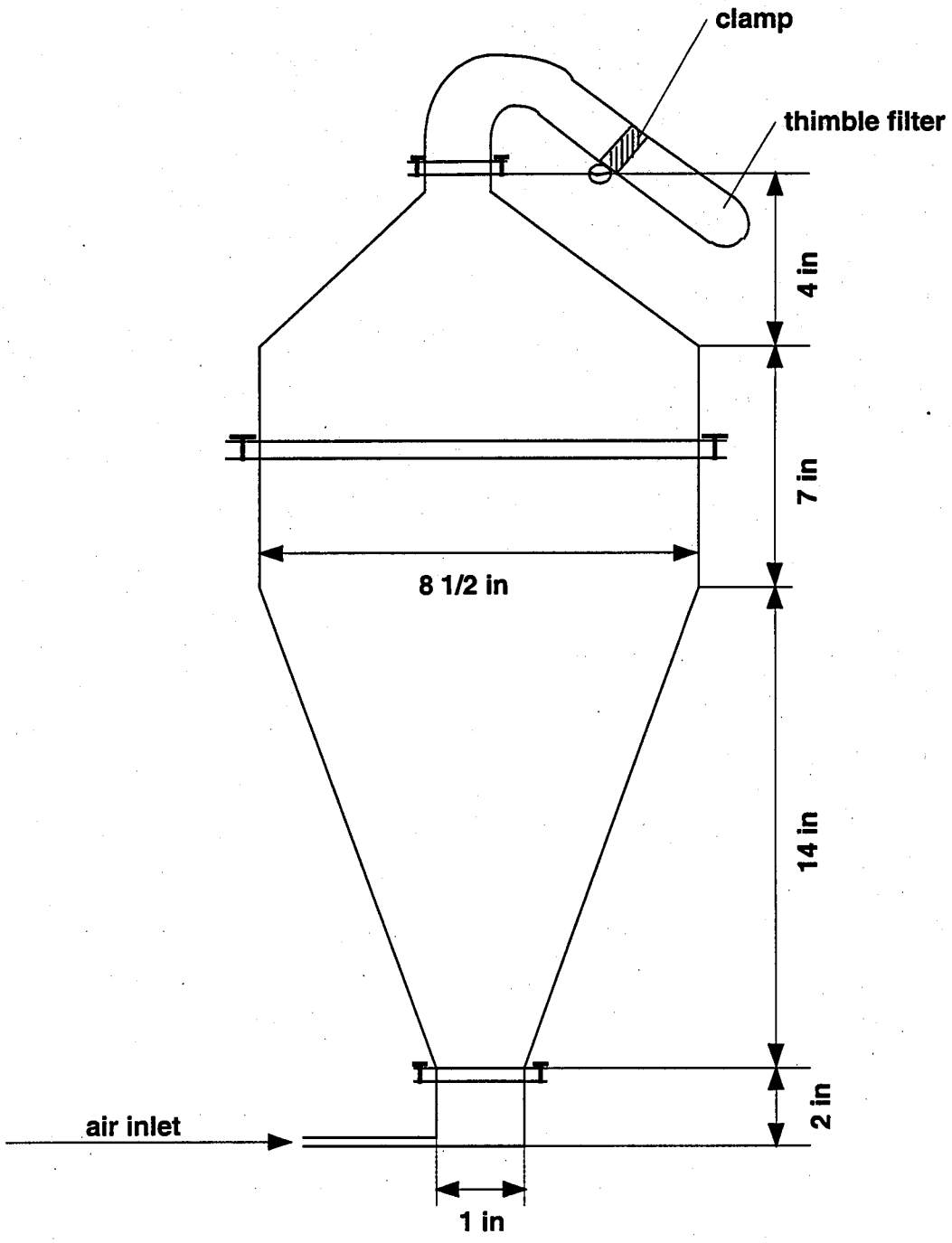

As illustrated in Figure 4, the ultrasonic system consisted of a 20 kHz Tekmar TM501 sonic disrupter with a CV26 horn and a 0.5 inch tip, a container for holding the catalyst slurry, and the horn support frame. Pre-weighed sample was dispersed in the media, which was distilled water in the present study, by stirring. Suspensions were prepared with about 2.5 vol% of solids in a total of 400 ml of distilled water [13,28,29]. The suspension was then treated at a particular energy setting of the sonic disrupter for 15 min. As reported by the system manufacturer, the maximum energy output is 500 W, and the settings correspond to percentages of the total energy output. In the present study, 150 W, 250 W, or 400 W energy settings were used. Since it was reported that temperature is one of the factors affecting ultrasonic energy output, a water bath was used in order to keep a relatively constant temperature of 23°C. After the electronic timer on the ultrasonic generator automatically shut down the system, the slurry was transferred, sampled and characterized using a particle size analyzer. The remainder of the slurry was filtered and dried at 110°C in an oven for SEM analysis.

2.3 Particle Analysis

A Leeds & Northrup Microtrac model 7990-11 laser particle size analyzer was used in order to measure the particle size distributions (PSDs). The original, fluidized bed, jet cup or collision test samples were each was put into 50 ml of deionized water and dispersed using an ultrasonic bath. The approximate 2.5 vol% suspension was then sampled for the Microtrac in order to determine PSD. The suspension from the ultrasonic test was stirred to an even distribution after the test before sampling. Samples were taken from the top, center and bottom of the suspension in order to ensure more accurate analysis. The results of several measurements of the same sample were averaged in order to minimize the error.

Figure 4. Ultrasonic system

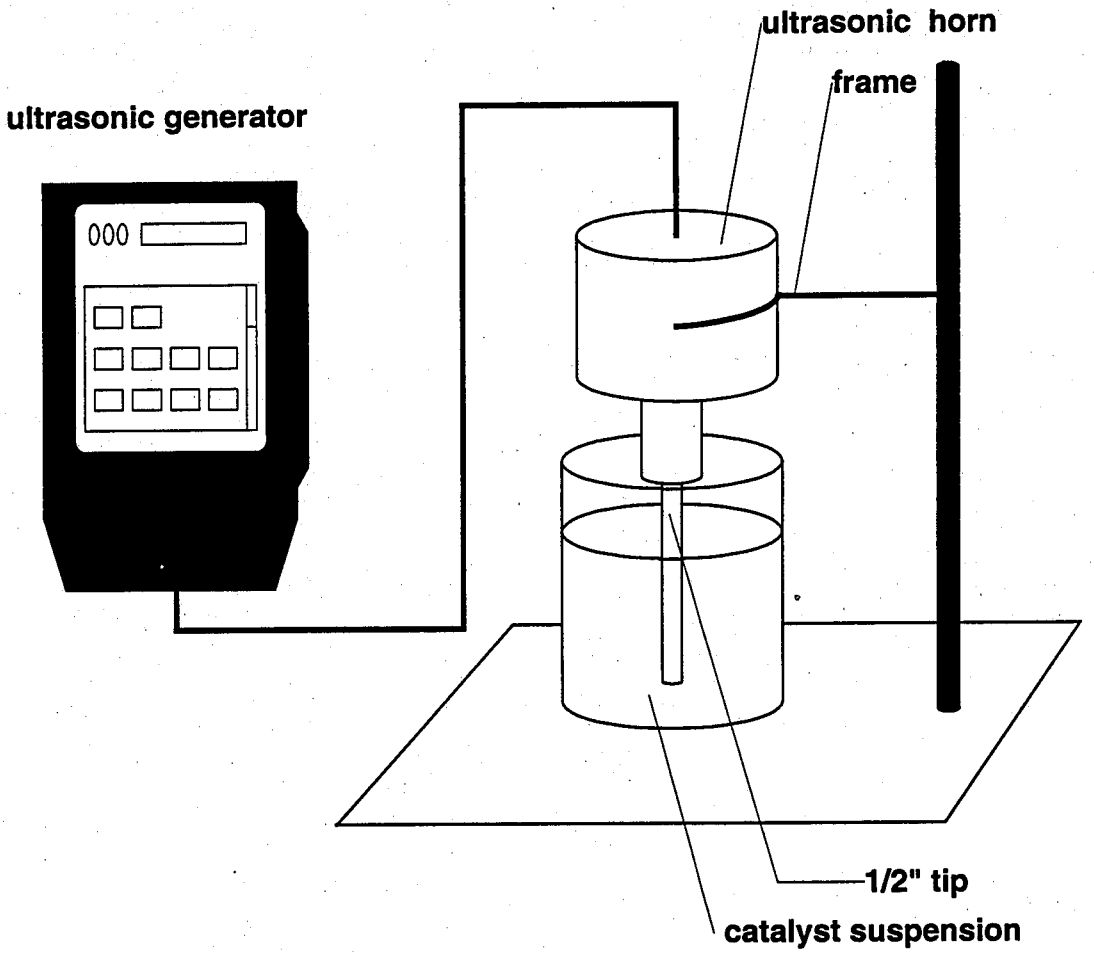

Since size distribution is usually plotted as weight (or volume) percentage versus average projected area diameter of particles in attrition studies, change in the volume moment, a type of average particle size commonly used to represent a particular PSD, has been selected as a useful indicator of the attrition process. The volume moment, x_{VM}, can be calculated by [32]:

$$x_{VM} = x_{WM} = \frac{\sum dM}{\sum dV} = \frac{\sum x^4 dN}{\sum x^3 dN} \quad (1)$$

where, x_{VM} is the volume moment, x_{WM} the weight moment, M the size moment, V the particle volume, and N the number of particles of size (diameter) x.

Particle morphology information was obtained for each sample by using a Philips XL30 FEG Scanning Electron Microscope (SEM). SEM micrographs were further analyzed using Scion Beta 2 image analysis software for determination of areas and perimeters of particle projections.

2.4 Reproducibility

Due to the limited amount of the Co/SiO_2 catalyst available, sieved Davison 952 silica support was used instead to evaluate the reproducibility of each test method. The comparisons are shown in Table 1. Weight percent elutriated and average particle size were used to determine the reproducibility of these attrition tests.

3. RESULTS

The morphology of the catalyst as prepared and sieved is showed in Figure 5. Although the silica support was spray dried, the catalysts as prepared were not as spherical as expected. This is considered to be due in part to particle agglomeration during catalyst preparation – as

Table 1. Reproducibility tests

Test	Run	Flow Rate	Time- on-Stream	Elutriated Fines (wt%)[a]	Volume Moment (μm)
Fluidized Bed	1	1.0 l/min	12 hr	10.85	70.1
	2	1.0 l/min	12 hr	10.39	70.7
	3	1.0 l/min	12 hr	11.17	69.8
Jet Cup	1	10 l/min	1 hr	17.0	46.8
	2	10 l/min	1 hr	18.6	45.2
	3	10 l/min	1 hr	17.0	44.2
Collision	1	1.0 l/min	1 time	NA	72.4
	2	1.0 l/min	1 time	NA	72.6
	3	1.0 l/min	1 time	NA	72.0
Ultrasound	1	250 W[b]	15 min	NA	48.1
	2	250 W[b]	15 min	NA	48.3
	3	250 W[b]	15 min	NA	48.8

a. Elutriated fines wt% = (weight of fines recovered from the fine recollection assembly after test/total weight of catalyst recovered after test) x 100%
b. Ultrasound energy setting: 50% of 500 W.

Figure 5. Morphology of the catalyst as prepared and sieved

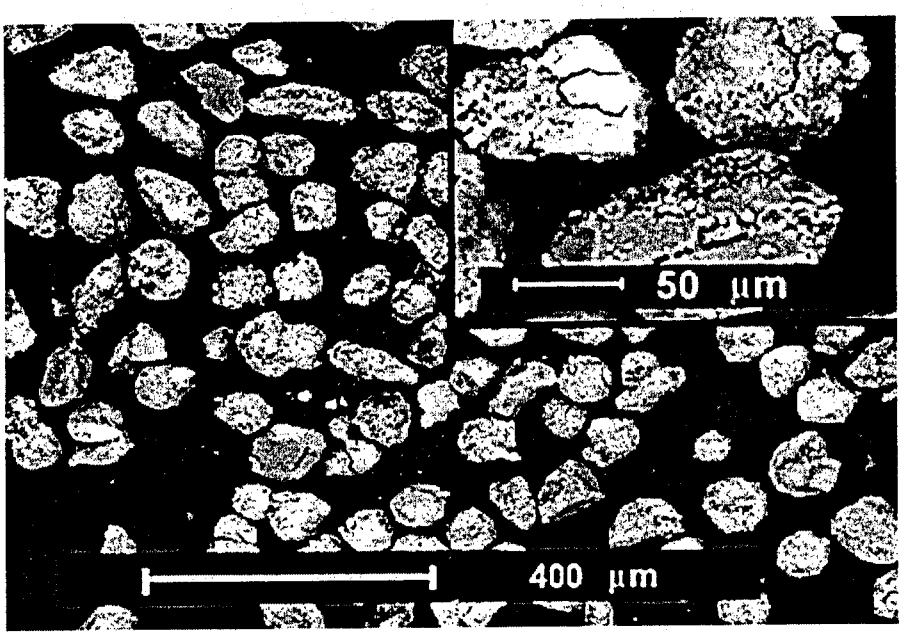

seen by comparing the particle morphology of pre-calcined and sieved catalyst support (Figure 6) and the Co catalyst after preparation (Figure 5). The catalyst support particles before preparation are relatively smaller and more spherical. On the other hand, in addition to particle agglomeration, some fracture and crack formation were also found on the catalyst particles after catalyst preparation. Some of the impregnated cobalt appeared to form cobalt patches on the surface of the silica support particles as can be seen in Figure 5. These patches were found both on and inside the silica support particles when space permitted and had an average size around 2 μm. They appeared at high magnification to be made up of clusters of Co oxide crystals (in the calcined catalysts).

As seen in the SEM micrograph (Figure 7), the catalyst particles after use in the SBCR appeared to be even less spherical than those of the catalyst as prepared (Figure 5). The number of broken particles (fragments and chips) obviously increased after FTS reaction in the SBCR. The external cobalt patches appeared not to be affected during the SBCR run. Obvious fractures could be observed for some of the larger particles. The PSDs of both fresh and used catalysts are given in Figure 8. Continuous curves, instead of bar charts, were chosen to represent the PSDs based on the assumption of continuous size distribution [30-32] for easier data comparison and analysis. The center size of each size interval (i.e., each Microtrac channel) was plotted as the abscissa and the frequency of particles in each interval as the ordinate. As shown in Figure 8, the average catalyst particle size decreased after use in the SBCR. The concentration of particles less than 30 μm obviously increased. Two peaks are apparent for the particles less than 30 μm in the PSD of the catalyst after SBCR use. Considering that fine particles were lost during the SBCR run through the liquid effluent filter with openings of 10 μm, the actual concentration of

Figure 6. Morphology of the catalyst support

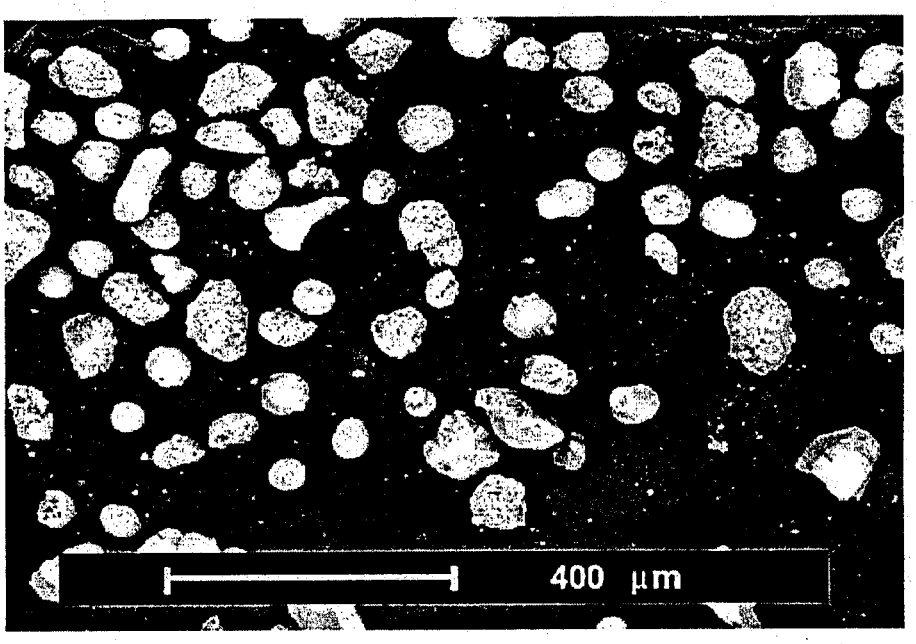

Figure 7. Morphology of the catalyst after SBCR FTS

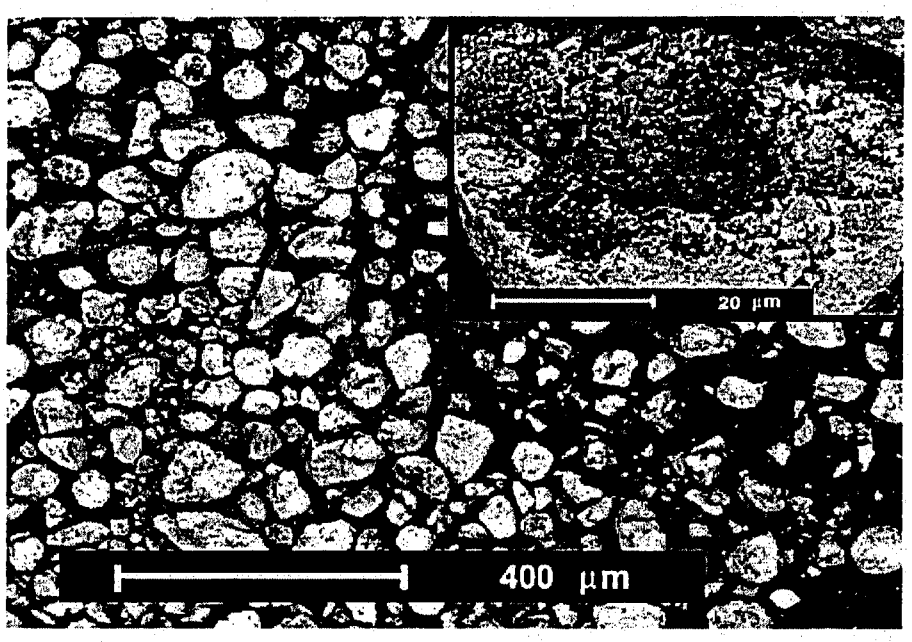

Figure 8. Comparison of PSD before and after the SBCR run

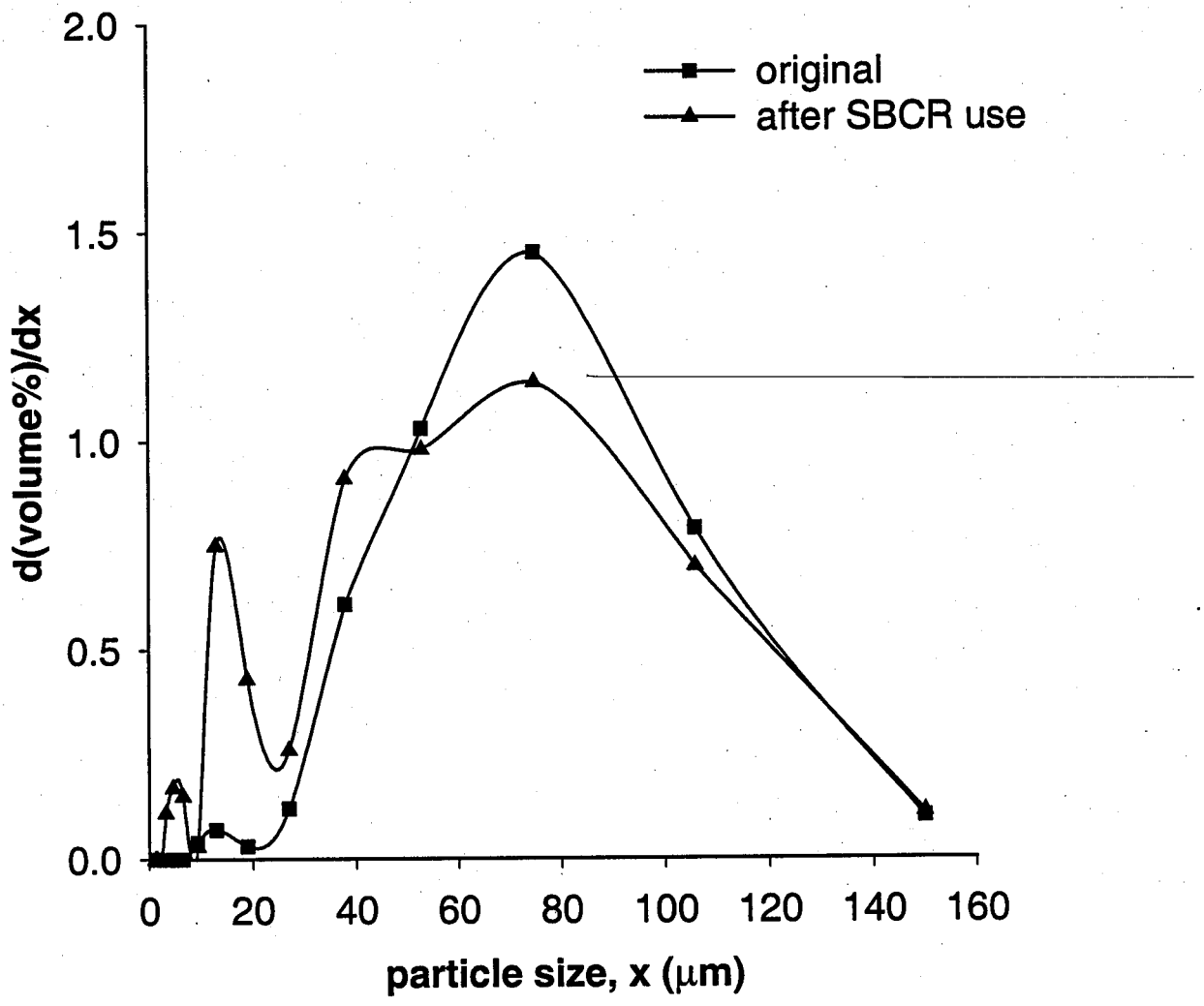

fine particles less than 10 μm should be higher. For particles larger than 30 μm, the PSD of the catalyst after SBCR use appears to have a bi-modal distribution as opposed to the essentially single modal distribution of the catalyst as prepared. Not only the average size, but also the concentration of these larger particles decreased during SBCR operation.

The attrition tests were run under various conditions and the resulting particle characteristics (from SEM) and size distributions were compared to those of the fresh catalyst and after the SBCR run. Figure 9 shows a comparison of the PSDs for the fluidized bed tests (after different lengths of testing time) with the PSDs for the catalyst as prepared and after the SBCR run. Due to the loss of most of fines <10 μm through the downstream filter during SBCR operation, all PSDs of the attrition test results were truncated to > 11 μm before being compared to the SBCR result. Note that all PSDs reported in this work include elutriated fines. The average particle size decreased with increasing time-on-stream in the fluidized bed. Both the weight percent of the elutriated fines (particles exiting the fluidized bed or jet cup and captured by the filter at the top of the system) and the volume moment, as well as other results, are summarized in Table 2. As can be seen by SEM, the particles remaining in the fluidized bed (Figure 10) were more spherical and/or smoother on the surface than those of the fresh catalyst (Figure 5). In addition, the number of cobalt patches on the outside surface of the catalyst particles was much less than that on the fresh catalyst particles. Particles elutriated (Figure 11) were less than 60 μm in size and included fragments and chips, as well as fines.

Similar results were found for the jet cup test. The particles remaining in the jet cup chamber (Figure 12) were more spherical compared to those of the fresh catalyst (Figure 5). However, the particles collected in the fines collection assembly of the jet cup test (Figure 13)

Figure 9. Comparison of PSD for the catalyst after the fluidized bed tests

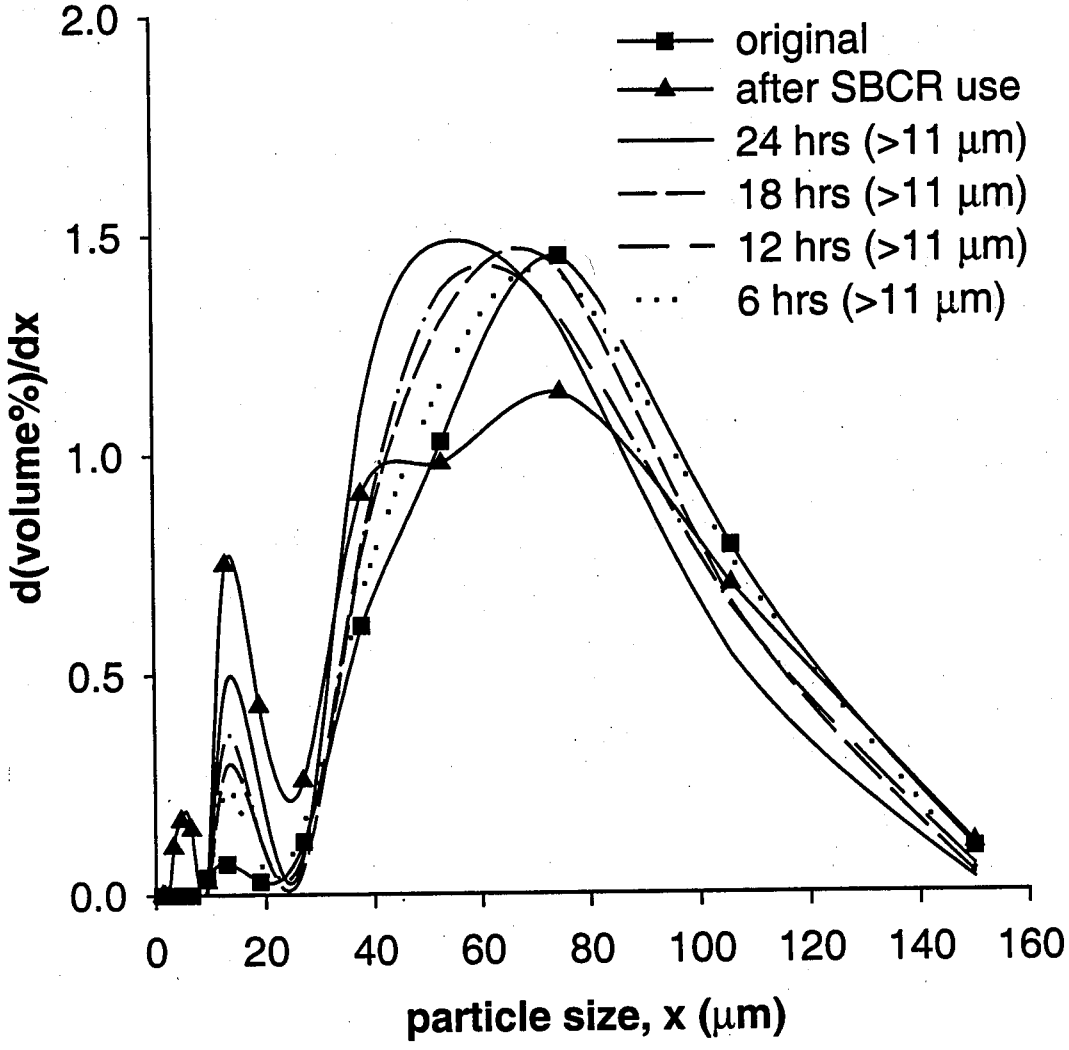

Table 2. Summary of attrition test conditions and results

Test	Flow Rate	Time-on-Stream	Elutriated Fines (wt%)	Volume Moment (μm)		Sphericity [a]	x_{g1}	x_{g2}	x_{g3}	x_{g4}	χ^2
				> 0 μm	> 11 μm						
Original Catalyst	NA	NA	NA	79.9	79.9	1.38	--	--	--	--	NA
After SBCR Run	NA	240 hr	NA	73.4	74.2	1.78	87.6	44.4	15.6	5.6	0.0
Fluidized Bed	1.5 l/min	6 hr	13.5	73.0	76.2	--	83.4	58.3	15.3	5.1	0.24
	1.5 l/min	12 hr	14.3	70.1	73.7	--	--	--	--	--	0.28
	1.5 l/min	18 hr	18.5	69.8	73.7	1.38	83.7	48.3	15.1	5.3	0.32
	1.5 l/min	24 hr	24.7	64.6	68.3	--	90.7	47.7	12.4	4.5	0.31
Jet Cup	10 l/min	1 hr	9.5	63.6	69.2	--	90.2	63.1	16.3	5.7	0.07
	15 l/min	1 hr	31.1	45.2	55.6	1.45	87.3	46.2	17.2	5.5	2.21
	20 l/min	1 hr	80.0	23.7	35.4	--	83.2	43.5	15.7	6.2	14.74
Collision	1.5 l/min	1 time	NA	78.7		--	--	--	--	--	0.45
	1.5 l/min	2 times	NA	78.3		1.36	83.8	52.5	16.0	--	0.35
	1.5 l/min	3 times	NA	78.6		--	--	--	--	--	0.47
Ultrasound	**150 W**	15 min	NA	73.7	73.7	--	86.9	59.5	15.0	2.8	0.42
	250 W	15 min	NA	63.3	65.5	1.46	85.3	55.1	15.3	4.6	0.28
	400 W	15 min	NA	61.4	64.2	--	89.0	55.0	14.5	5.1	0.32

a. sphericity=(circumference)^2 /4π*(projection area of particle outline)

$$\chi^2 = \sum_{i=1}^{k} \frac{(Observed - Expected)^2}{Expected}$$

Figure 10. SEM of the catalyst particles remaining in the fluidized bed (24 hrs time-on-stream)

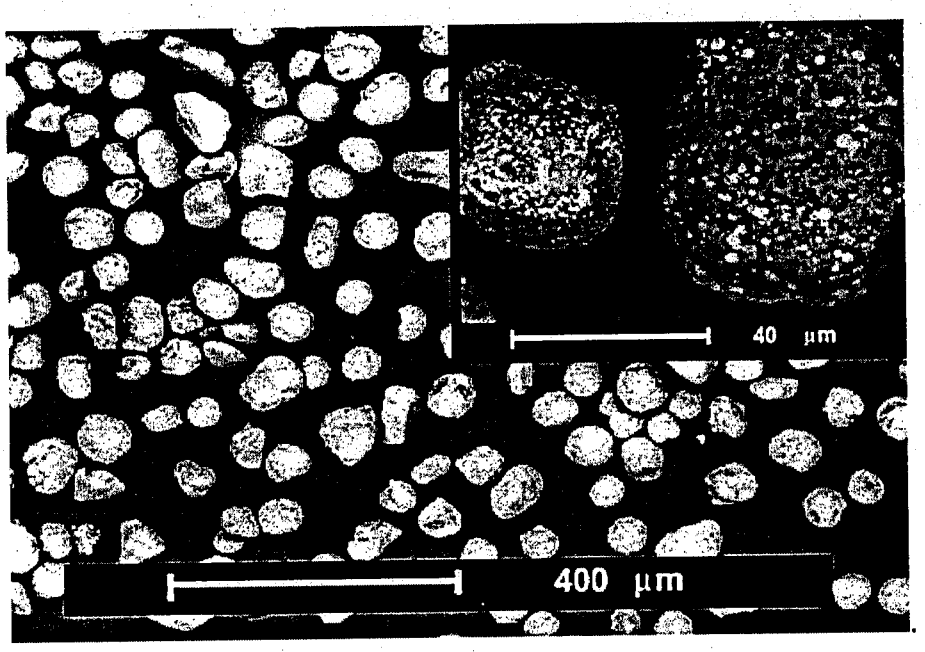

Figure 11. SEM of the elutriated fines of a fluidized bed test recovered in the fines collection assembly (24 hrs time-on-stream)

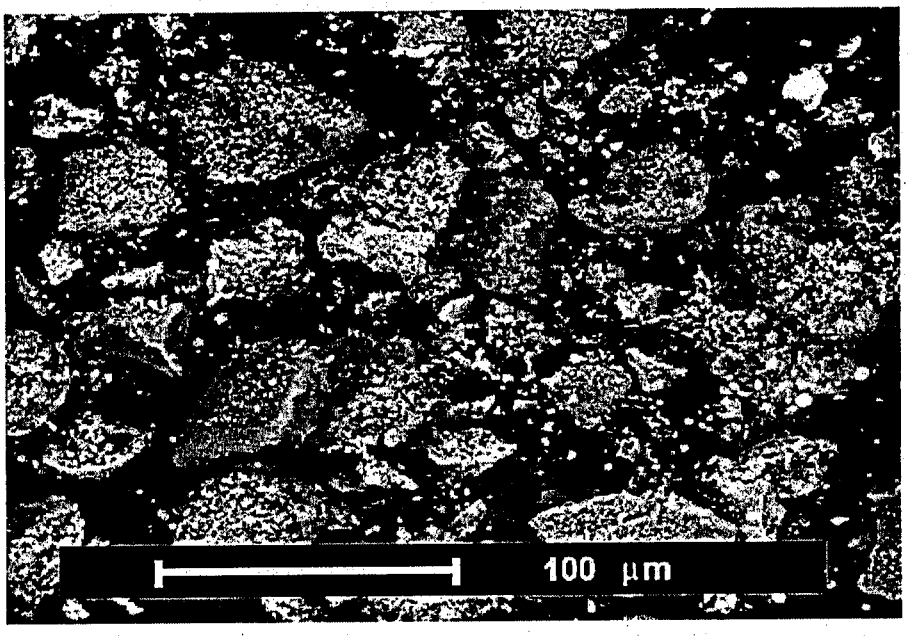

Figure 12. SEM of the catalyst particles remaining in the jet cup chamber (15 *l*/min flow rate)

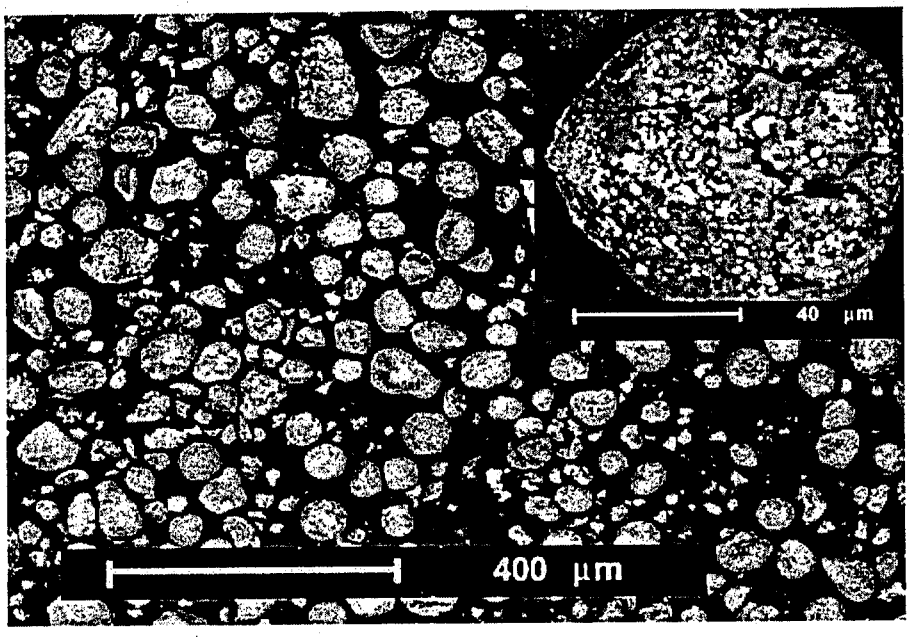

Figure 13. SEM of the fines in the fines collection assembly of a jet cup test 915 *l*/min flow rate)

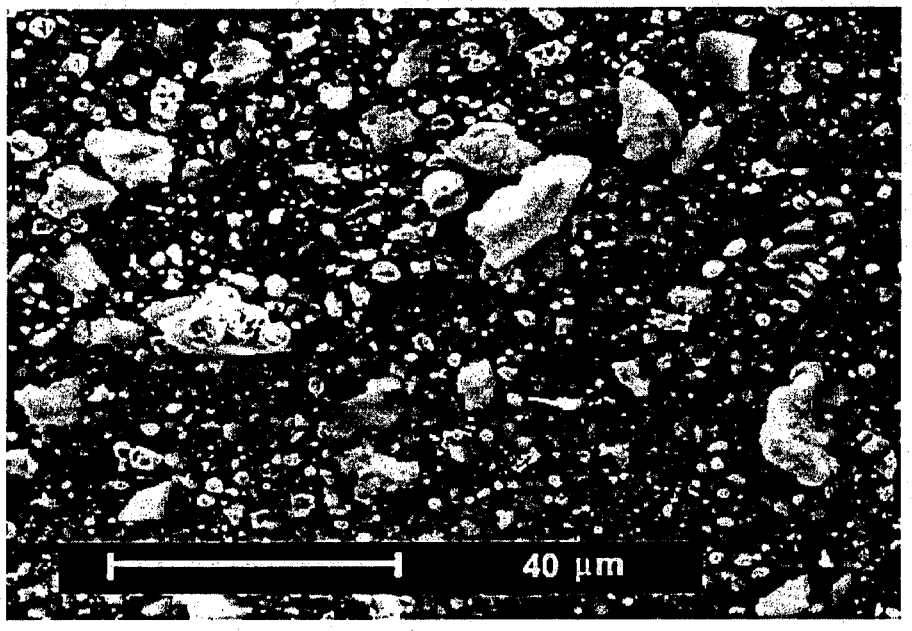

were smaller than for the fluidized bed, mostly chips and fines due to the different fluidization conditions (such as system configuration, flow rate, etc.) in the jet cup. No fragments larger than 30 μm were observed in the fines collected. In Figure 14, the PSDs following several 1 hr jet cup tests using different flow rates are plotted with the distributions of the fresh and the SBCR used catalyst. It is apparent that the mean particle size decreased with an increase in the flow rate.

Different from the results for the fluidized bed and jet cup tests, the change in mean particle size (volume moment) in the collision test, another air jet type test, was small even after multiple runs. The PSDs for different numbers of runs are plotted in Figure 15 and are very close to the PSD of catalyst as prepared. No particles less than 16 μm were observed. The morphology of the catalyst particles recovered after 2 sequential collision tests is illustrated in Figure 16. As expected, the particles after the collision test were similar to those of the fresh catalyst in morphology but contained slightly more chips. The cracks and fracture on larger catalyst particles were also more obvious than those on the fresh catalysts.

The ultrasonic test was the only test employed in the present study that did not involve a high velocity air jet but rather ultrasound. The breakdown of particles is believed to be caused by cavitation via the expansion and subsequent intense collapse of tiny bubbles in the liquid medium [28,29]. The PSDs resulting from different ultrasonic power settings are plotted in Figure 17. It is apparent that the degree of change in mean particle size increased with an increase in ultrasound power setting (or in other words power input), but this trend is not linear with the power input. The PSDs of the catalyst after testing were very close for the runs at power settings of 250 W and 400 W. The morphology of the particles after a 15 min ultrasonic

Figure 14. Comparison of PSD after the jet cup tests

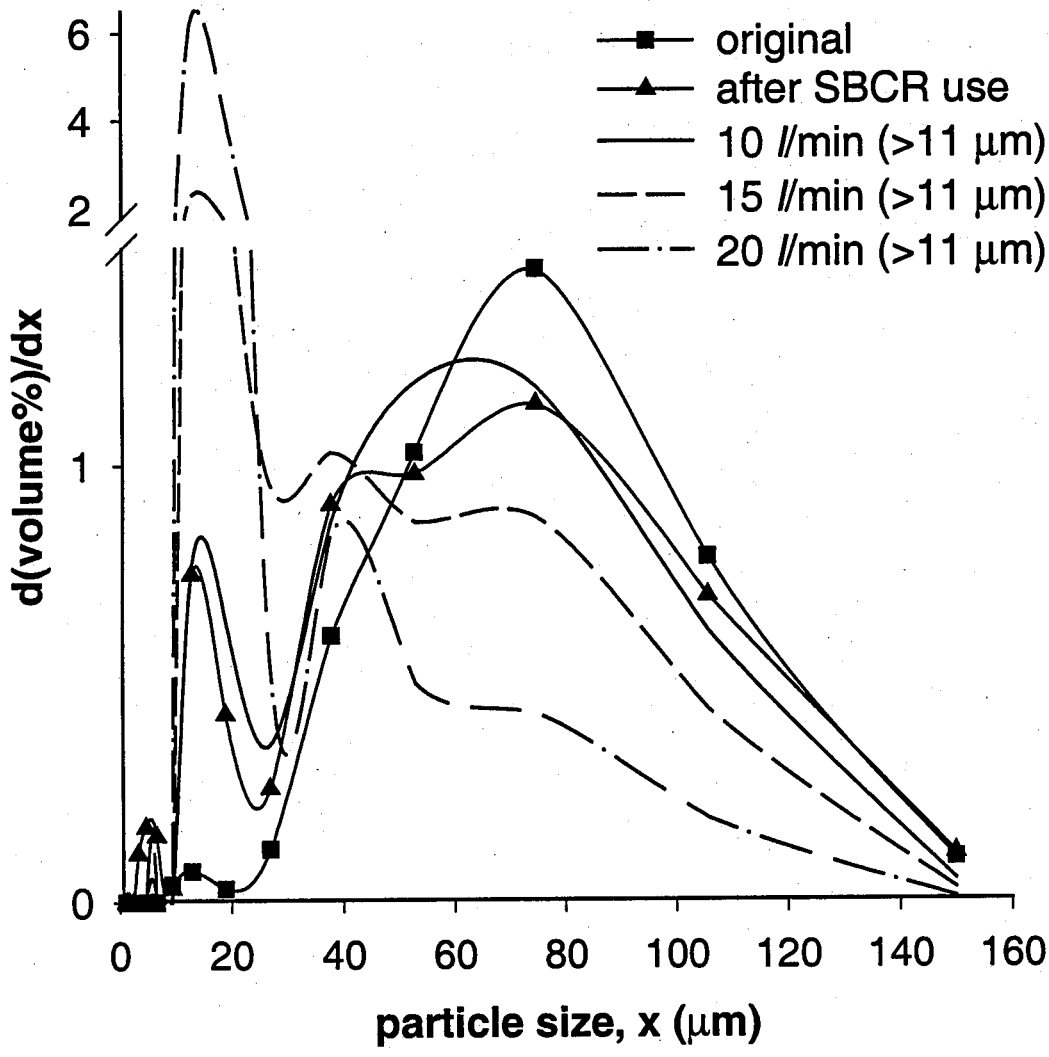

Figure 15. Comparison of PSD after the collision tests

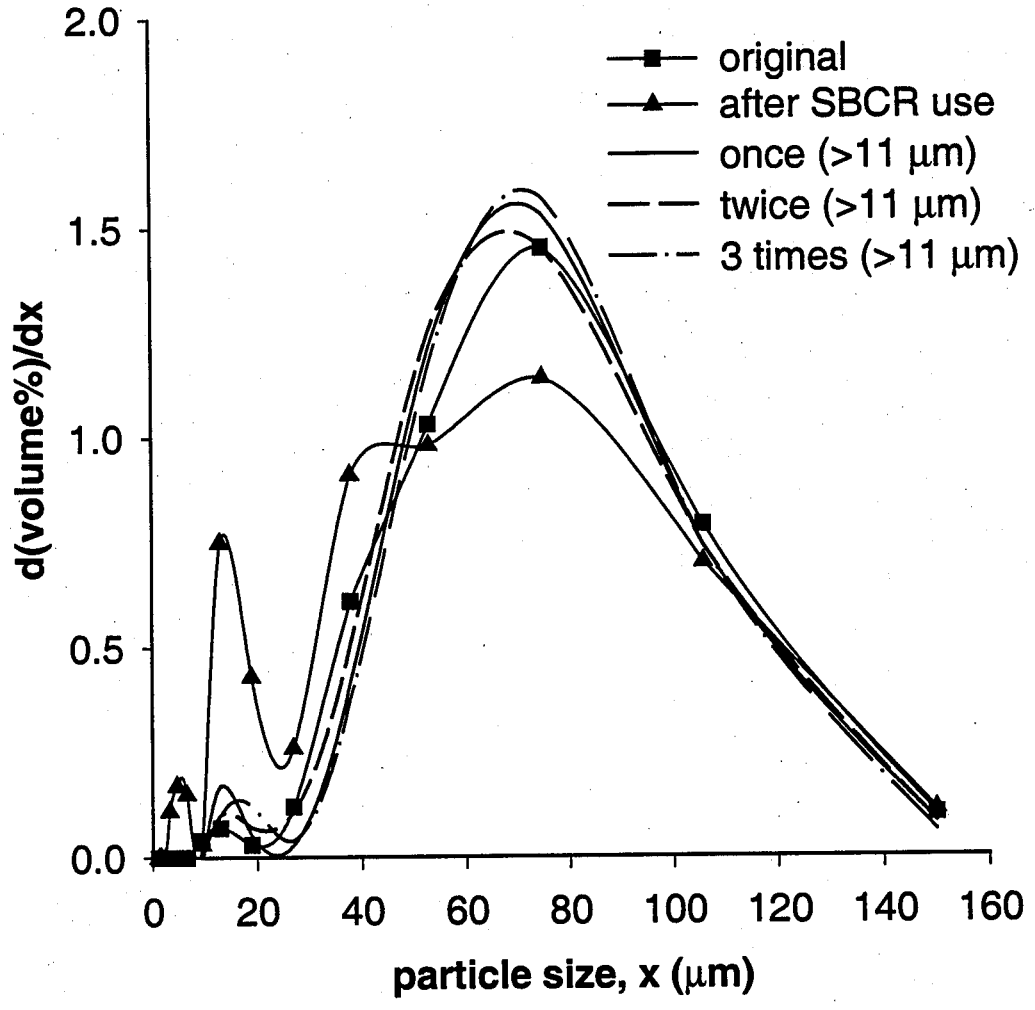

Figure 16. SEM of catalyst particles after a collision test (twice)

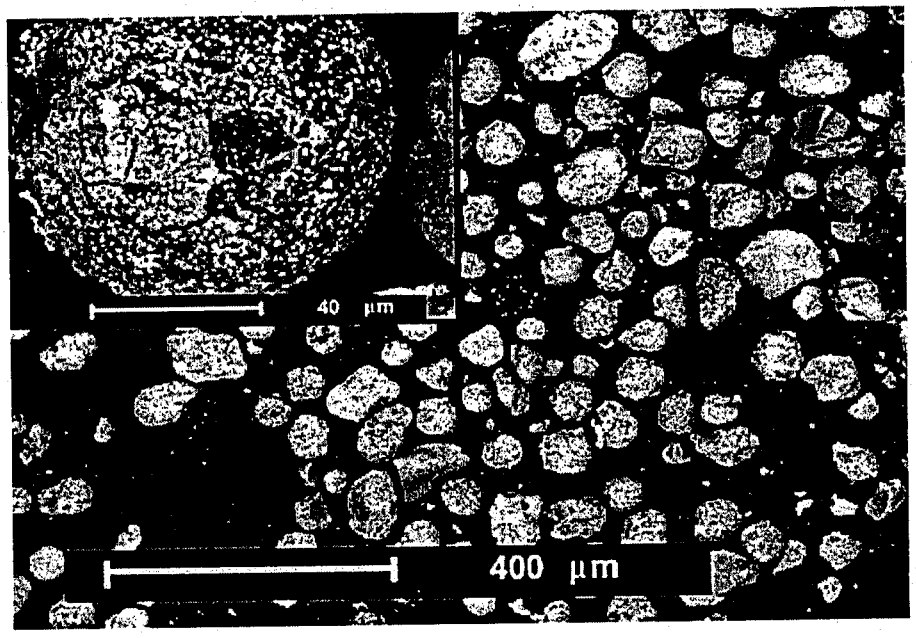

Figure 17. Comparison of PSD after ultrasound tests

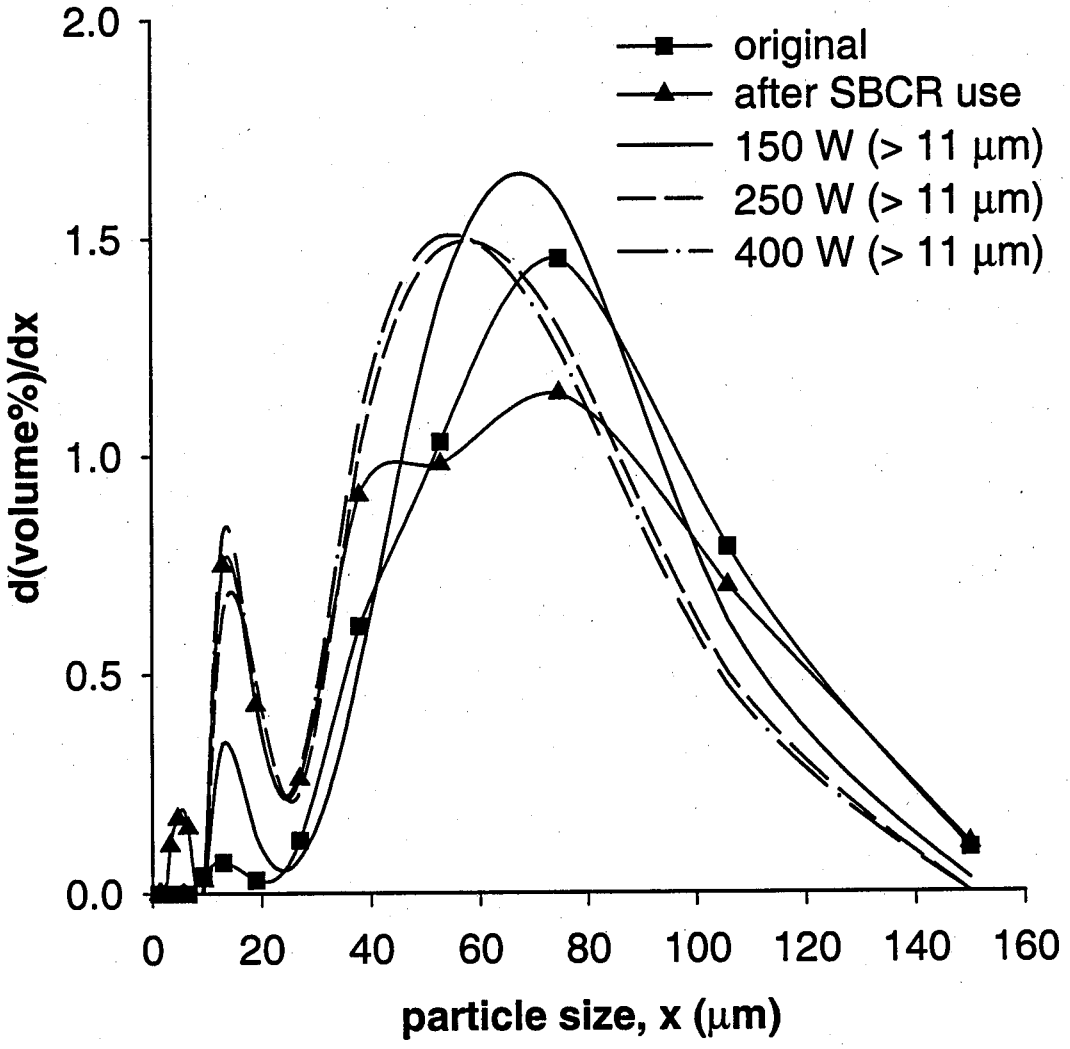

test at a power setting of 250 W is illustrated in Figure 18. The particles are apparently more spherical than those of the catalyst as prepared. Particle breakage may have been a result of crack propagation under pressure, rather than pure impact fractures.

4. DISCUSSION

4.1 Attrition Mechanisms in the SBCR

SEM provides a very powerful and direct determination of attrition mechanism since it is easy to distinguish broken particles resulting from abrasion or fragmentation based on particle morphology. Catalyst particles after the SBCR run (Figure 7) were much less spherical compared to the fresh catalyst (Figure 5). Compared to the fluidized bed and jet cup test results (Figures 10 & 12), surface layer removal was not evident for the SBCR sample (Figure 7) and cobalt patches on the catalyst surface were similar to those of the original catalyst (Figure 5). It is, therefore, speculated that the presence of the dense molten wax served as a "lubricant" between particles during the SBCR run and reduced the abrasion by a considerable degree. In order to quantify the particle morphology, the average particle sphericity was calculated based on the Scanning electron micrographs

$sphericity = (particle \quad circumference)^2 / (4\pi \times particle \quad projection \quad area)]$. The sphericity value for a spherical particle is 1, and this value increases with an increase in particle irregularity. As shown in Table 2, catalyst particles apparently were much less spherical after the SBCR run. This evidence suggests that the mechanisms of chipping and fragmentation, therefore, may have been the primary cause of attrition in the SBCR.

Figure 18. SEM of catalyst particles after an ultrasonic test (250 W power input)

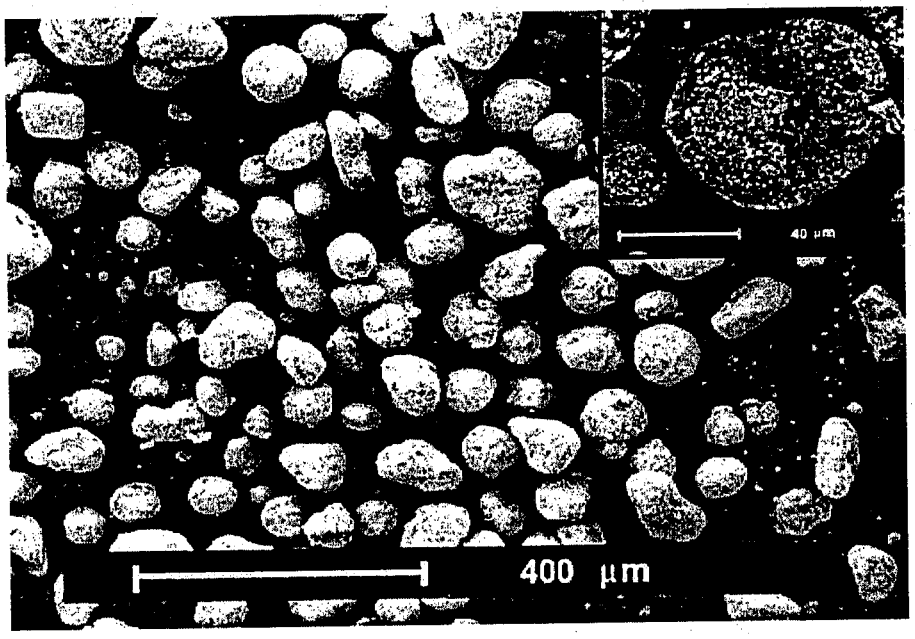

4.2. Attrition Mechanisms in the Attrition Tests

For the fluidized bed, jet cup and ultrasonic tests (Figures 10, 12, & 18), the large catalyst particles remaining were obviously smoother on the surface and more spherical compared to the fresh ones (Figure 5), which suggests that abrasion was much more important than during the SBCR run. Image analysis of these micrographs indicates that samples after the fluidized bed, jet cup and ultrasonic tests did not show any significant change in sphericity (Table 2). This might have been caused by the inclusion of the smaller and irregular fragments during image analysis. For fluidized bed and jet cup, only the SEM micrographs for the particles remaining in the chamber were used for image analysis. Since most of the fragments and chips were elutriated out in the fluidized bed, the sphericity value after this test was found to be relatively lower compared to that after the jet cup test. The higher sphericity value of the jet cup is considered to be partly due to the inclusion during image analysis of considerable amounts of fragments. For the ultrasound test, since all the particles were used for image analysis, a higher sphericity value was also observed.

While abrasion is more apparent for the fluidized bed, jet cup and ultrasound tests compared to that in the SBCR, it could not account for all the attrition. Instead, chipping and fragmentation both must exist in order to achieve the observed particle size reduction. Evidence of the existence of chips and fragments can be seen in the results after fluidized bed, jet cup and ultrasound tests (Figures 10-13, & 18).

It is obvious that the collision test is a different attrition process than the other three methods. As expected, since fracture is the dominant mechanism in this type of test, catalyst particles were less spherical (Figure 16) compared to those after the fluidized bed and jet cup tests (Figures 10 & 12). For the collision test, the change in volume moment was insignificant even after several consecutive runs (Table 2), although chips and small fragments can be

observed in the SEM micrograph (Figure 16). Perhaps only a few flawed particles broke or Microtrac measurement is unable to detect particle change if only a corner of a particle is broken off. This supports the suggestion [16] that there is a necessary velocity required for the threshold of significant particle breakage.

4.2 Comparison of the Different Attrition Tests

It has been shown above that the attrition processes in these tests differ somewhat from each other and also from that of the SBCR run. However, the goal of this work is not to find a test (or a specific experimental condition) that necessarily generates exactly the same attrition result as the 240 hr laboratory SBCR run, since application of a catalyst in a different SBCR would produce different attrition results. Rather, it is to determine a laboratory scale test that is able to reasonably mimic the attrition processes in an SBCR in order to predict the relative attrition resistances of different catalysts developed for SBCR use. Thus, a single attrition parameter cannot define an adequate attrition test. Instead, it is a combination of such parameters that can suggest a suitable test. The various attrition parameters are compared below.

The weight percent of elutriated fines (ratio of weight of fines recovered to total weight of catalyst recovered) was measured for both fluidized bed and jet cup tests and is listed in Table 2. The weight loss of elutriated fines increased with increase in time-on-stream for the fluidized bed test and with the increase in flow rate for the jet cup test, consistent with earlier reports [11,12,33]. In most attrition tests, the weight percent of elutriated fines is used as the sole measure of attrition. It is suggested that such a single measure, while giving a quick result, is inherently flawed due to the fact that elutriation rate is determined by many parameters, such as particle density and shape. In addition, due to different fluidization conditions, it is very difficult to use weight percentage of elutriated fines for comparison between the fluidized bed and jet cup

tests. Moreover, it is impossible to compare such results for these two tests with those of the ultrasonic test, the collision test, or the SBCR run, for which an amount of elutriated fines cannot be measured. Furthermore, similar to other reports [4,11], the attrition rate (weight of fines elutriated per unit time) in the fluidized bed test was found to decrease with time-on-stream, whereas the attrition rate in the jet cup test was relatively constant during the short period of testing (1 hr).

As shown in Table 2, the change in volume moment indicates that all the tests except the collision test were able to generate considerable attrition in relatively short periods of time. The volume moment value determined for the catalyst after the SBCR run is somewhat higher than the actual value since fines lost through the 10 μm filter were not included in the calculation. Thus, to provide a more exact comparison, the values of volume moment for the PSDs truncated at 11 μm are also listed in Table 2 for the SBCR run and all the tests. By comparing these volume moment values, three of the attrition tests can be considered to be reasonable in terms of producing attrition. For the 15 min ultrasonic (at 150 W power input), 1 hr jet cup (at 10 *l*/min flow rate), and 18 hr fluidized bed tests, the volume moments of the catalyst particles decreased approximately the same amount as that for the 240 hr SBCR run. The jet cup and ultrasonic tests appeared to be more aggressive in producing attrition in a shorter time than the fluidized bed test.

The PSDs can be further analyzed in order to determine the suitability of these tests in predicting SBCR attrition. Log-normal is the most commonly used distribution function for particle size in powder technology. In past studies, log-normal distribution was used to describe both the original and the resulting PSDs [32]. It has also been modified to describe samples of truncated or mixed particles [32, 33]. In the present study, a multi-model log-normal distribution was used to fit the experimental data. Considering the attrition mechanisms and the SEM results,

it was assumed that four different types of particles (unbroken/slightly broken particles, fragments, chips and fines) resulted during attrition. Therefore, a quad-model log-normal distribution as given by equation (2) was used to describe the catalyst particles after the SBCR run and attrition tests.

$$\frac{d\phi}{d\ln(x)} = \sum_{i=1}^{k} \frac{P_i}{\sqrt{2\pi}\ln(\sigma_{gi})} \exp\left[-\frac{\{\ln(x)-\ln(x_{gi})\}^2}{2\ln^2(\sigma_{gi})}\right] \qquad (2)$$

Where, ϕ is the general term for the frequency and volume percentage in this present study, σ_{gi} is the standard deviation for each peak, P_i is the percentage of each peak in the overall distribution, x_{gi} is the mean (or center) size of each peak, and x is the particle size. This distribution model fits the experimental data quite well (see Figures 19 and 20). The center values of each peak for the log-normal distributions are also listed in Table 2. The quad-model distribution was not used to deconvolute the PSD of the fresh catalyst because the catalyst as prepared and sieved consisted only of unbroken particles. Although there are only fifteen data points available for the Microtrac results for each sample, this deconvolution analysis is still considered applicable due to the good reproducibility of the Microtrac data points. However, the exact location of the peaks should be considered to be only approximate. As can be seen from Table 2, the center values for x_{g3} and x_{g4} are very similar for all the attrition tests and the SBCR run. Considering the SEM results, this might be a confirmation of the assumed existence of fines and chips (due to abrasion and chipping mechanisms). For the collision test, there was no

Figure 19. Curve fit of the results for the SBCR run

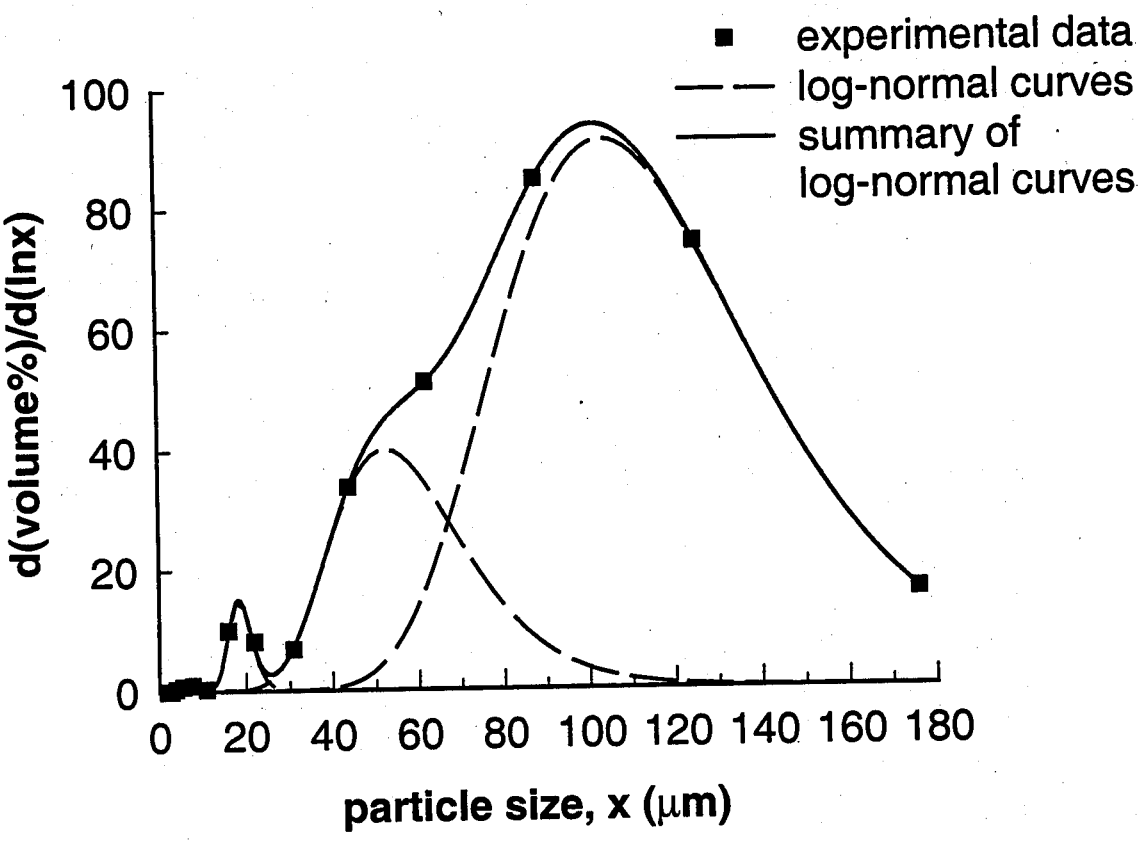

Figure 20. Curve fit of the results for the fluidized bed test for 24 hours time on stream

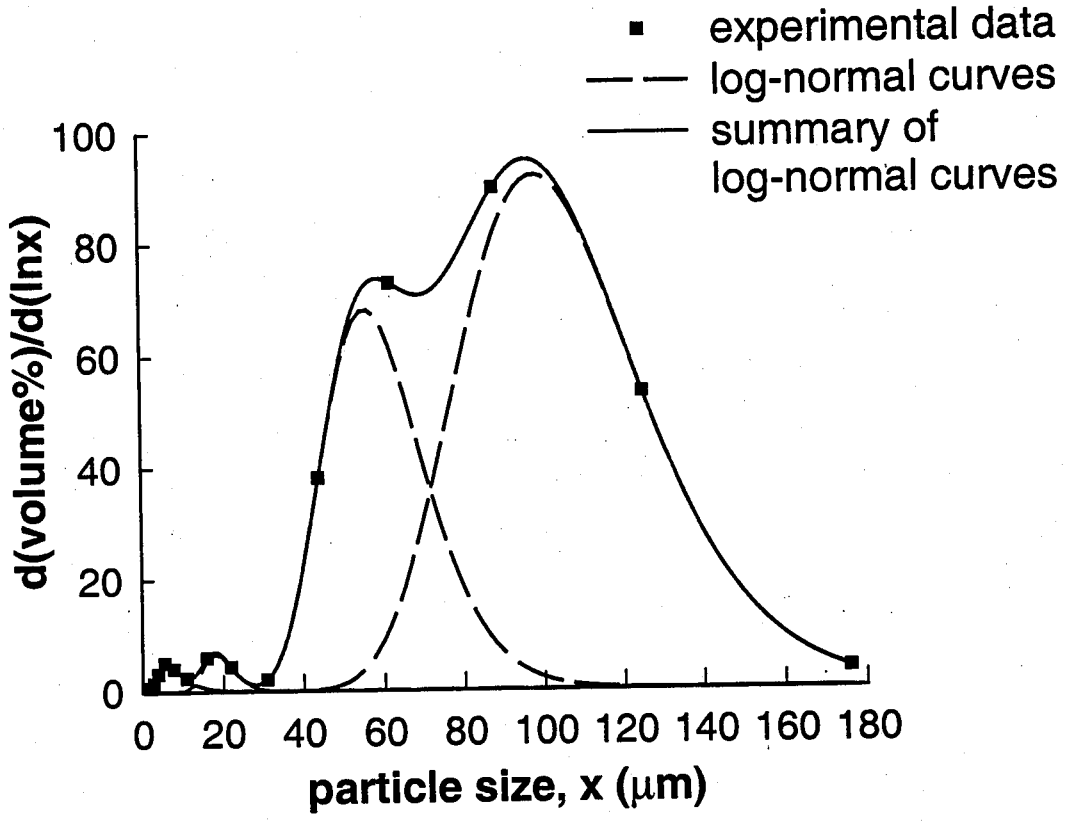

obvious peak for the fines (x_{g4}), suggesting that little abrasion occurred during the particle breakdown. However, the x_{g1} and x_{g2} of the different tests varied significantly. This is considered to be partly due to errors caused by the few data points available in the large particle size range. This difference is also probably partly due to differences in the fracture and abrasion mechanisms for the different tests. It seems that the x_{g2} value after the SBCR run was relatively lower than that after most of the tests. This might be a result of more fragmentation attrition during the SBCR run.

A Chi-squared (χ^2) test [35] was employed to determine the statistical goodness of fit for the PSDs after the various test methods to the PSD after the SBCR run. The χ^2 results are listed in Table 2 for all the tests. The closer the value of χ^2 is to 0, the better the goodness-of-fit and the better the test generated result matches the SBCR result. Only the jet cup test at 10 *l*/min showed near perfect fit. Other jet cup tests at higher flow rate deviated greatly due to aggressive attrition and the high concentration of fines generated. The PSDs from the fluidized bed tests showed poorer fits than the 10*l*/min jet cup test. The χ^2 value for the PSD's after the fluidized bed and ultrasound tests were similar and, as to be expected, better somewhat than those after the collision tests.

5. Conclusion

It was observed that catalyst attrition in a laboratory SBCR run differs somewhat from that in the attrition tests studied. Attrition in the SBCR and the collision test appeared to be fracture dominant, while abrasion was not very important. In the fluidized bed, jet cup, and ultrasound tests, abrasion was more important than in the SBCR, but fragmentation and chipping

also obviously occurred in order to give the particle size distributions (PSDs) which resulted. Although there are some differences in the attrition processes in different systems, the objective of this research was to determine a laboratory scale attrition test which is able to evaluate in a timely fashion the relative attrition resistances of different catalysts developed for SBCR use, rather than to produce exactly the same attrition result as a particular laboratory SBCR run. Therefore, the comparisons of attrition resulting from the different tests and the SBCR run focused on the overall suitability of these tests in mimicking the attrition in the SBCR, especially with regards to the PSD.

Since a single attrition parameter cannot define an adequate attrition test, various attrition parameters were compared. Among the parameters considered, attrition efficiency, i.e, the attrition generated during a certain period of time, was obvious an important criteria for determining the suitability of a test. Although the attrition mechanisms in the collision test appeared to be similar to that of the SBCR run, its attrition efficiency was too low to be suitable for testing attrition. On the contrary, obvious decreases in average particle size were obtained after fluidized bed, jet cup, and ultrasound tests. Using optimum operating conditions, all three tests produced attrition results in terms of change in average particle size, PSD, and % fines quite similar to that produced in the SBCR. Thus, all three tests can be used to study the relative attrition resistance of catalysts developed for SBCR usage. However, the jet cup (10l/min., 1 hr) can be considered slightly superior to the other two based on and in-depth analysis of PSD.

Reference

1. British Materials Handling Board, "Particle Attrition, State-of-the Art Review", Trans Tech, Germany, 1987.
2. Bemrose, C.R., and Bridgwater, J., Powder Tech., 49 (1987) 97.
3. Forsythe, W.L. Jr., and Hertwig, W.R., Ind. Eng. Chem., 41 (1949) 1200.
4. Gwyn, J.E., AIChE Symposium Series, 15 (1969) 35.
5. Zenz, F.A., Hydrocarbon Processsing, 50 (1971) 103.
6. Zenz, F.A., Hydrocarbon Processing, 53 (1974) 119.
7. Wei, J., Lee, W.Y., and Krambeck, F.J., Chem. Eng. Sci., 32 (1977) 1211.
8. Cairatl, L., Dl Flore, L., Forzatti, P., Pasquon, I., and Triflro, F., Ind. End. Chem. Process Des. Dev., 19 (1980) 561.
9. Vaux, W.G., and Fellers, A.W., AIChE Symposium Series, 77 (1981) 107.
10. Pedersen, L.A., Lowe, J.A., and Matocha, C.K., Sr., in "Characterization and Catalyst Development: an Interactive Approach", American Chemical Society, Washington DC, 1989, p. 414.
11. Weeks, S.A., and Dumbill, P., Oil and Gas J., 88 (1990) 38.
12. Werther, J., and Xi, W., Powder Tech., 76 (1993) 39.
13. Kalakkad, D.S., Shroff, M.D., Kohler, S., Jackson N., and Datye, A.K, App. Catal. A, 133 (1995) 335.
14. Fletcher, R., Oil and Gas J., 93 (1995) 79.
15. Srinivasan, R., Xu, L., Spicer, R.L., Tungate, F.L., and Davis, B.H., Fuel Sci. Tech. Int., 14 (1996) 1337.
16. Yuregir, K.R., Ghadiri, M., and Clift R., Powder Tech., 49 (1986) 53.
17. Cleaver, J.A.S., and Ghadiri, M., Powder Tech., 76 (1993) 15.

18. Ghadiri, M., in "Powder Technology Handbook, 2nd Edition", Marcel Dekker, New York, 1997, p. 283.

19. Beaver, E.R., AIChE Symposium Series, 70 (1974) 1.

20. ASTM D-4058-92, Standard Test Method for Attrition and Abrasion of Catalyst and Catalyst Carriers.

21. Dolling, P.K., Gainer, D.M., and Hoffman, J.F., J. of Testing and Evaluation, 21 (1993) 481.

22. Matocha, C.K., Sr., Crooks, J.H., and Plazio, P.P, in "Light Metals", AIME, New York, 1987, p. 129.

23. Matocha, C.K., Sr., and Crooks, J.H, in "Light Metals, Addendum", AIME, New York, 1987, p. 875.

24. ASTM D5757-95, Standard Test Method for Determination of Attrition and Abrasion of Powdered Catalysts by Air Jets.

25. Saxena, S.C., Catal. Rev. Sci. Eng., 37 (1995) 227.

26. Bhatt, B.L., Heydorn, E.C., and Tijm, P.J.A., in "Proceedings of the 1997 Coal Liquefaction & Solid Fuels Contractors Review Conference", US Department of Energy, Federal Energy Technology Center, Pittsburg, Pennsylvania, 3-4 September, 1997, p. 41.

27. Geanskoplis, C.J., in "Transport Processes and Unit Operations, 2nd Ed.", Allyn and Bacon, Boston, 1983, p. 134.

28. Thoma, S.G., Douglas, M.S., and Ciftcioglu, M., Powder Tech., 68 (1991) 53.

29. Thoma, S.G., Douglas, M.S., and Ciftcioglu, M., Powder Tech., 68 (1991) 63.

30. Austin L.G, Powder Tech., 5 (1971) 1.

31. Yu, A.B., and Standish, N., Powder Tech., 62 (1990) 101.

32. Allen T., in "Particle Size Measurement, 5th ed.", Chapman & Hall, New York, 1997, p. 45.

33. Ray, Y.C., Jiang, T.S., and Wen, C.Y., Powder Tech., 49 (1987) 193.

34. Inga, J.R., Ph.D. Dissertation, University of Pittsburgh, Pittsburgh, 1997.

35. Holman, J.P., in "Experimental Methods for Engineers, 3rd Edition", McGraw-Hill, New York, 1978, p. 51.